Supplement to
HESS Opinion: Floods and droughts - Land use, soil management, and landscape hydrology are more significant drivers than increasing temperatures

Karl Auerswald[1], Juergen Geist[1], John N. Quinton[2], Peter Fiener[3]

[1]School of Life Sciences, Technical University of Munich, Freising, 85354, Germany
[2]Lancaster Environment Centre, Lancaster University, Lancaster, LA1 4YQ, UK
[3]Working Group Water and Soil Resource Research, University of Augsburg, Augsburg, 86159, Germany

Correspondence to: John Quinton (j.quinton@lancaster.ac.uk)

1. Description of the example area

1.1 Landscapes

Bavaria, a federal state in the south of Germany, is 70550 km² in size and larger than about half of the countries in the European Union e.g. the Netherlands or Ireland (BStMWi, 2023). Geologically and geomorphologically, it can be separated into four zones (Ahnert, 1989). (1) In the south, there is the narrow strip of the German Alps, with the highest elevation being 2962 m a.s.l. (2) Adjoining to the north is the hilly Alpine Foreland. It ends at the River Danube, which crosses Bavaria from the west to the east. (3) North of the Danube is the cuesta landscape of the Mesozoic Scarpland. Most of this area drains to the River Main, a tributary of the River Rhine. The lowest point of Bavaria can be found in the north-west where the Main leaves Bavaria (about 100 m a.s.l.). (4) In the east, Bavaria is bordered by crystalline mountain ridges that are part of the Bohemian Massif (highest elevation 1458 m a.s.l.).

Loess-influenced soils are widespread except in the Bohemian mountain ridge and the Bavarian Alps. The loess deposits can be several meters deep in the east along the River Danube and in the north of the Mesozoic Scarpland. However, more commonly, the loess cover has a depth of one meter or less, making soil fertility vulnerable to soil losses by erosion.

1.2 Climate

The Köppen-Geiger climate zones change from Cfb (temperate oceanic) in the northwest to Dfb (humid continental with warm summer) in the south. Dfc (continental subarctic climate) or ET (tundra climate) can be found at high altitudes.

The weather and hydrological data, covering the period 1951 to 2015, were taken from Baumeister et al. (2017), who applied a hydrological model (GWN-BW) that is particularly designed to calculate groundwater recharge. Like almost all hydrological models, the model considers only coarse land-use classes and not accounting for the changes that occurred within the land uses. Furthermore, it does not consider lateral interactions between land uses (e.g., oasis and clothesline effects on evapotranspiration, run-on infiltration, and interflow). Hence, the model results almost entirely depict meteorological changes in space and time.

Annual rainfall in Bavaria increases from about 600 mm yr^{-1} in the north to about 1400 mm yr^{-1} in the Bohemian Massif in the east and to more than 2000 mm yr^{-1} in the Alps in southern Bavaria. The overall spatio-temporal mean for Bavaria is 938 mm yr^{-1}.

Actual evapotranspiration in Bavaria is approximately 500 mm yr^{-1} (overall mean 528 mm yr^{-1}), with higher values south of the Danube (mainly around 600 mm yr^{-1}), where sunshine duration is more prolonged (Klämt, 2008). In forests, evaporation in the south can even be around 700 mm yr^{-1}.

Total runoff (direct runoff and groundwater recharge; overall mean 409 mm yr^{-1}) reflects the pronounced gradient in precipitation, given that the variation in evapotranspiration is comparably small. For most of the country, total runoff varies between 200 and 400 mm yr^{-1} but decreases to 100 to 200 mm yr^{-1} in lowland areas that receive less rainfall (rain shadow) and experience higher temperatures and higher radiation (foehn effect). In particular, this is the case near the river Main and also in a 20 to 50 km wide belt south of the River Danube. High total runoff can be expected at high elevations, in particular in the Alps, where total runoff may even exceed 1500 mm yr^{-1}.

About half of the total runoff is groundwater recharge (overall mean 206 m yr^{-1}), and the other is direct runoff (overall mean 204 mm yr^{-1}). Both components have a similar spatial pattern as total runoff and vary between 50 and 600 mm yr^{-1} depending on the region. A distinct deviation from this 50:50 ratio can only be found in the karst areas of the Mesozoic Scarpland, where a larger fraction of total runoff is allocated to groundwater.

The changes during the last seven decades have been pronounced for air temperature but minor for other meteorological and hydrological variables (Fig. A1). Annual mean temperature has risen from about 7.5°C to 9°C. Temperatures started to change circa 1980 and increased almost linearly until 2015. Spatially, this increase was uniform.

The temporal changes in precipitation, evapotranspiration, direct runoff, and groundwater recharge were minor compared to the spatial variation and without a clear trend. Between 1950 and 2015, groundwater recharge decreased by a total of 22 mm yr^{-1} (i.e., on average, it decreased by 0.33 mm yr^{-1} every year during the last 65 years), and actual evapotranspiration decreased by a total of 7 mm yr^{-1}, while precipitation decreased by a total of 53 mm yr^{-1}. These changes occurred spatially relatively uniformly, implying that the relative changes were larger in the drier areas.

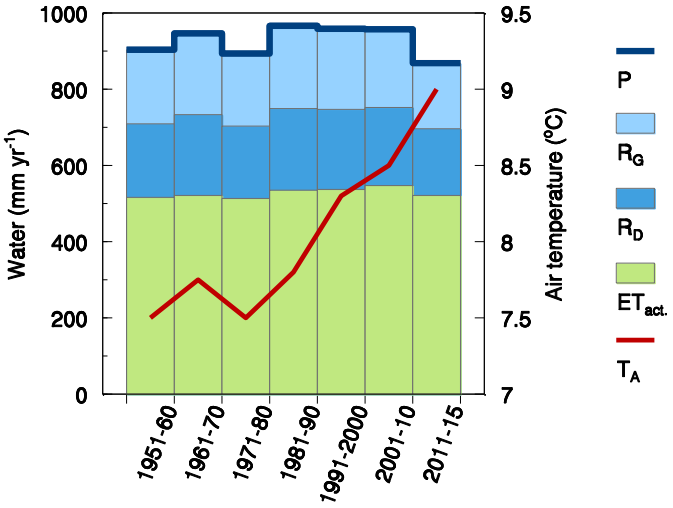

Figure A1: Change in air temperature (T_A), falling precipitation (P), evapotranspiration (actual ET_{act}), direct runoff (R_D), and groundwater recharge (R_G) during the past seven decades and averaged over entire Bavaria (data compiled from Baumeister et al., 2017).

1.3 Land use

Population density is 190 km^{-2} (total population: 13.4 million; BStMWi, 2023). Settlement and traffic area covers 12%, while forests contribute 37%, farmland 43%, and water bodies 2% (the missing area is unused land, mainly in the Alps, and other miscellaneous parts). Two-thirds of the farmland is cropland; one-third is grassland. Grain crops contribute 53% to the cropland, 29% are fodder crops (mainly silage maize), and 5% are row crops (except silage maize). The most important crop is winter wheat, followed by silage maize. About 30% of the agricultural area is cropped by farms 50 to 100 ha in size. About 50 % of the farmland is leased (Bayerisches Landesamt für Statistik, 2023).

The changes in land use during the last seven decades (Fig. A2) falsely indicate that forests and cropland hardly changed in terms of their percentage contribution, yet, grassland has decreased, and settlement and traffic areas continuously increased (Fig. A2). In reality, forests have become heavily fragmented, particularly by infrastructure projects. Although the lost forest area has been compensated at the expense of cropland and grassland, the forests have become cut in small pieces (for an example see Auerswald et al., 2019a), changing their hydrological behavior (increasing the clothesline effect, increasing drainage by roadside ditches).

Cropland has experienced the most significant losses. In particular, the best loessal soils and the flat areas were preferred construction sites. The hydrologic change is thus more pronounced than the aerial change because the loss predominantly occurred on soils with high water storage capacity and low surface runoff.

The loss of cropland is not evident from the overall numbers illustrated in Fig. A2 because it was compensated by converting grassland into cropland. This loss of grassland did not happen evenly but predominantly affected the grassland interspersed in cropland. These were wet depressions that were drained, riparian grassland where the groundwater was lowered, or the

grassland previously occurring along thalwegs (nowadays called grassed waterways when established by technical engineering). This interspersed grassland had traditionally been the fodder base for mixed farms. Thus, alongside the loss of grassland, an increase in fodder production on cropland occurred, namely silage maize. Note that the loss of grassland is almost perfectly mirrored by the rise in maize (Fig. A2). The loss of the interspersed grassland, combined with replacing organic with mineral fertilizers, allowed specialization of farms either focusing on animal production or cash crops. Again, this loss of grassland was hydrologically more critical than the loss of aerial share suggests because the wet places in the landscape became drained. Also, the areas predominantly contributing to run-on infiltration, the grassed thalwegs, disappeared. Increasing maize acreage promoted runoff, erosion, and soil evaporation in early summer, when maize cover is still sparse.

The loss of grassland has stopped in recent years because the conversion of grassland to cropland has been forbidden since 2019, although its conversion to settlement area would still be allowed. This conversion ban has caused the cropland to decrease since then because the losses of cropland to urban development cannot be compensated anymore by grassland conversion. This also illustrates that urban development predominantly ocured on cropland.

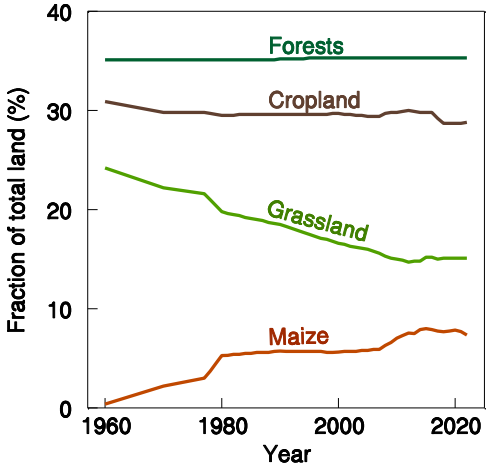

Figure A2: Contribution of forests, cropland, grassland, and maize to total land in Bavaria during the past six decades. The maize area is included in the cropland area. The data were compiled from different official sources. The settlement area is displayed in Fig. A3.

The areas of settlements and roads more than doubled during the past five decades (Fig. A3) and at a rate which is increasing. The sealing ratio, i.e., the fraction of the settlement and traffic area that cannot infiltrate anymore, is also increasing. The increase in the sealing ratio applies not only to the new settlement and traffic areas but to the total area covered by buildings and roads. This indicates that sealing continues on old settlement and traffic areas, e.g. by increasing the building density and sealing the open spaces to create parking lots.

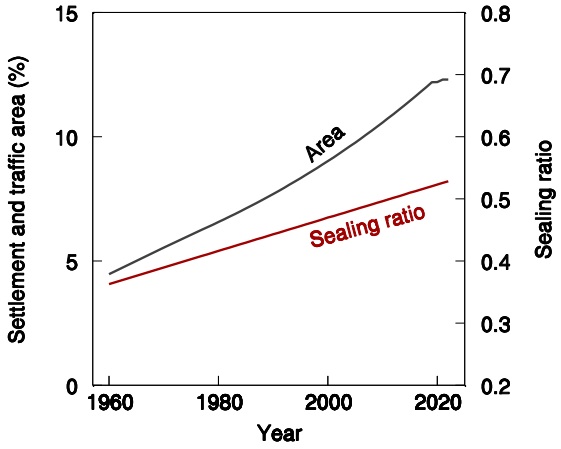

Figure A3: Increase in settlement and traffic area in Bavaria during the past five decades and sealing ratio of the settlement and traffic area. The data on settlement area were mainly taken from https://www.stmuv.bayern.de/themen/boden/flaechensparen/daten.htm; those on the sealing ratio were adopted from https://www.lfu.bayern.de/umweltkommunal/flaechenmanagement/bodenversiegelung/index.htm.

2 Prediction of surface runoff and rain erosivity from climate projections for Bavaria

We used an ensemble of 10 climate projections from the EURO-CORDEX initiative (Jones et al., 2011; Knist et al., 2017) for the period 1970 to 2050 based on the RCP 8.5 scenario reflecting business as usual (Table A1). These projections were approved by the Deutscher Wetterdienst (German Weather Service) (Hübener et al., 2017). The data had a resolution of 0.11° (approximately 12.5 km), and they covered Bavaria, the hydrological catchment of Bavarian rivers, and a 50 km buffer area, thus extending to substantial parts of Austria, Switzerland, Italy, and the Czech Republic. The climate projections delivered daily air temperatures and daily precipitation.

Predicting runoff from daily precipitation was straightforward using the SCS curve number model (Woodward et al., 2002; NRCS, 2004). According to present land use, curve numbers for different crops, land uses, and hydrologic soil groups were taken from Seibert and Auerswald (2020). They were kept constant for the projection period to isolate precipitation effects from other effects. Any errors in the assumption of curve numbers will have a minor impact because we were only interested in the relative change of runoff, not its absolute amount. Nevertheless, Seibert and Auerswald (2020) have shown that these curve numbers adequately reflected runoff of 1174 events from 22 catchments in Bavaria ranging from 12 to 170 km² in size. The calculation of rain erosivity, which depends on rain amount and rain intensity, requires higher resolved rainfall than the daily rainfall available from climate projections. Considering the pronounced influence of air temperature on precipitation rate (Lenderink and van Meijgaard, 2008), a strong correlation between event erosivity, calculated from highly resolved rain gauge data, and daily air temperature and daily precipitation could be established from 605738 erosive events and validated by another 15133 events from an independently measured data set (erosivities of both data sets were taken from Fischer et al., 2018;

Figure A4). The correlation yielded the following transfer function (Eq. 1) between event erosivity (called erosion index *EI* in N h^{-1}), daily precipitation (P_d in mm d^{-1}) and daily mean air temperature (T_a in degree Celsius).

$$EI = 1.57 \times 10^{-6} \times P_d^{2.63} \times T_a^{2.52} \quad (1)$$

Training data and testing data used event erosivities because event erosivities cannot be split between days, while daily values were used for rainfall and temperature. In cases, where an event extended over more than one day, the data of the day with the largest rainfall were used. In consequence, the equation returns event erosivities. The discrepancy between event rainfall and daily rainfall contributes to scatter in the transfer function, but its overall effect should be accounted for by the equation.

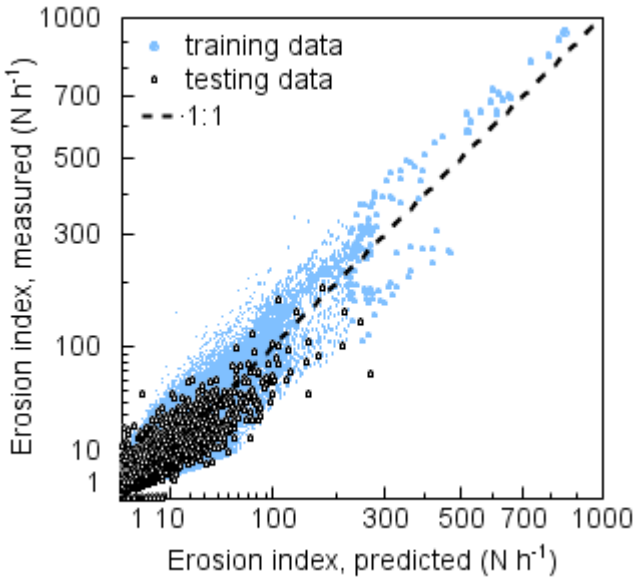

Figure A4: Transfer function to derive rain erosivity (erosion index) from climate projections: Correlation of the measured erosion index with a prediction using the measured daily amount of rain and the daily air temperature (adopted from Auerswald et al., 2019d). The axes are square root scaled. The unit N h^{-1} can be converted to MJ mm ha^{-1} h^{-1} by multiplying by 10.

In addition to the agreement with the validation data, the spatial pattern of rain erosivity and the interannual pattern of rain erosivity, when applying the transfer function to the climate projection data of the 1970s, agreed with the published map and interannual variation of rain erosivity from rain gauge measurements in Bavaria (Rogler and Schwertmann, 1981). Also, the trend in rain erosivity calculated rain from climate projections yielded a similar behavior for the period covered by measurements (1970-2022; measured data were taken from Auerswald et al., 2019b;c; Winterrath et al., 2023), although both data sets were determined independently and used different data. Specifically, the measured erosivities did not use daily air temperature and daily precipitation but temporarily highly resolved rain data. For the years 1970 to 2016, these data were

obtained from rain gauge measurements, while from 2001 to 2022, rain radar data (5 min resolution) for ca. 350000 locations were used (Auerswald et al., 2019b).

More details of the climate projections and the development of the transfer function can be found in Auerswald et al. (2019c).

Table A1: Euro-Cordex climate models approved by the German Weather Service were used to model future erosivity and runoff. For abbreviations see Hübener at al. (2017).

Number	General circulation model (GCM)	Institution	Regional climate model (RCM)	Driving ensemble member
2	CNRM-CM5	Centre National de Recherches Meteorologiques	ALADIN53	r1i1p1
4	EC-EARTH	EC-EARTH Consortium	KNMI-RACMO22E	r1i1p1
6	EC-EARTH	EC-EARTH Consortium	CCLM 4-8-17	r12i1p1
7	EC-EARTH	EC-EARTH Consortium	SMHI-RCA4	r12i1p1
9	IPSL-CM5A-MR	Institut Pierre-Simon Laplace	SMHI-RCA4	r1i1p1
12	HadGEM2-ES	Met Office Hadley Centre	SMHI-RCA4	r1i1p1
13	MPI-ESM-LR	Max Planck Institute for Meteorology	CCLM 4-8-17	r1i1p1
14	MPI-ESM-LR	Max Planck Institute for Meteorology	REMO2009	r1i1p1
15	MPI-ESM-LR	Max Planck Institute for Meteorology	SMHI-RCA4	r1i1p1
16	MPI-ESM-LR	Max Planck Institute for Meteorology	REMO2009	r2i1p1

References

Ahnert, F. (Ed.): Landforms and Landform Evolution in West Germany, Catena Supplement, 15, Cremlingen, Germany, 347 p., 1989.

Auerswald, K., Moyle, P., Seibert, S. P., and Geist J.: HESS opinions: Socio-economic and ecological trade-offs of flood management – benefits of a transdisciplinary approach, Hydrol. Earth Syst. Sc., 23, 1035–1044, https://doi.org/10.5194/hess-23-1035-2019, 2019a.

Auerswald, K., Fischer, F.K., Winterrath, T., and Brandhuber, R.: Rain erosivity map for Germany derived from contiguous radar rain data, Hydrol. Earth Syst. Sc. 23, 1819–1832, https://doi.org/10.5194/hess-23-1819-2019, 2019b.

Auerswald, K., Fischer, F., Winterrath, T., Elhaus, D., Maier, H., and Brandhuber, R.: Klimabedingte Veränderung der Regenerosivität seit 1960 und Konsequenzen für Bodenabtragsschätzungen, [Climate-change-induced changes in rain erosivity and consequences of soil loss estimation (in German)], in: Bodenschutz, Ergänzbares Handbuch der Maßnahmen und Empfehlungen für Schutz, Pflege und Sanierung von Böden, Landschaft und Grundwasser (Loseblattsammlung), edited by: Bachmann, G., König, W., Utermann, J., Berlin, Erich Schmidt Verlag, 4090, 21 p., 2019c.

Auerswald K., Fischer F., Winterrath T.: R-Faktor – Regenerosivität, in: Pilotstudie „Klimawirkungskarten Bayern“. UmweltSpezial, Bayerisches Landesamt für Umwelt, Augsburg, 61-69, 2019d.

Baumeister, C., Gudera, T., Hergesell, M., Kampf, J., Kopp, B., Neumann, J., Schwebler, W., and Wingering M.: Entwicklung von Bodenwasserhaushalt und Grundwasserneubildung in Baden-Württemberg, Bayern, Rheinland-Pfalz und Hessen (1951-2015), [Development of soil hydrology and groundwater recharge Baden-Wuerttemberg, Bavaria, Rhineland-Palatinate and Hesse (in German)], KLIWA-Berichte 21, 102 pp., https://www.kliwa.de/_download/KLIWAHeft21.pdf, last access: 08 March 2024, 2017.

BStMWi: Bayerns Wirtschaft in Zahlen 2023. Bayerisches Staatsministerium für Wirtschaft, Landesentwicklung und Energie, https://www.stmwi.bayern.de/publikationen/detail/pub-bayerns-wirtschaft-in-zahlen-2023/, last access 08 March 2024, 2023.

Bayerisches Landesamt für Statistik: Bodennutzung der landwirtschaftlichen Betriebe in Bayern 2022. https://www.statistik.bayern.de/mam/produkte/veroffentlichungen/statistische_berichte/c1102c_202200.pdf; last access 07 March 2024, 2023

Fischer, F.K., Winterrath, T., Auerswald K.: Temporal- and spatial-scale and positional effects on rain erosivity derived from point-scale and contiguous rain data, Hydrol. Earth Syst. Sc., 22, 6505–6518, https://doi.org/10.5194/hess-22-6505-2018, 2018.

Hübener, H., Bülow, K., Fooken, C., Früh, B., Hoffmann, P., Höpp, S., Keuler, K., Menz, C., Mohr, V., Radtke, K., Ramthun, H., Spekat, A., Steger, C., Toussaint, F., Warrach-Sagi, K., and Woldt, M.: ReKliEs-De Regionale Klimaprojektionen Ensemble für Deutschland, [ReKliEs-De Regional climate projections ensemble for Germany (in German)], https://doi.org/10.2312/WDCC/ReKliEsDe_Ergebnisbericht, 2017.

Jones C., Giorgi F., Asrar G.: The coordinated regional downscaling experiment: CORDEX, an international downscaling link to CMIP5, Clivar Exchanges, 16, 34-40, 2011.

Klämt, A.: Langzeitverhalten von Sonnenscheindauer und Globalstrahlung sowie von Verdunstung und Klimatischer Wasserbilanz in Baden-Württemberg und Bayern, KLIWA-Berichte 12, 147 pp., https://www.kliwa.de/_download/KLIWAHeft12.pdf, last access: 08 March 2024, 2008.

Knist, S., Goergen, K., Buonomo, E., Christensen, O. B., Colette, A., Cardoso, R. M., Fealy, R., Fernández, J., García-Díez, M., Jacob, D., Kartsios, S., Katragkou, E., Keuler, K., Mayer, S., van Meijgaard, E., Nikulin, G., Soares, P. M. M., Sobolowski, S., Szepszo, G., Teichmann, C., Vautard, R., Warrach-Sagi, K., Wulfmeyer, V., and Simmer, C.: Land-atmosphere coupling in EURO-CORDEX evaluation experiments, J. Geophys. Res.-Atmos., 122, 79-103, https://doi.org/10.1002/2016JD025476, 2017.

Lenderink, G. and van Meijgaard, E.: Increase in hourly precipitation extremes beyond expectations from temperature changes, Nat. Geosci., 1, 511–514, https://doi.org/10.1038/ngeo262, 2008.

NRCS: Estimation of direct runoff from storm rainfall, in: National Engineering Handbook. Part 630 Hydrology, chapter 10, Natural Resources Conservation Service (NRCS), United States Department of Agriculture, pp. 79, 2004.

Winterrath, T.: Jährlicher (2001-2019) R-Faktor [N/h/yr] auf Basis der stündlichen Niederschlagszeitreihen der RADKLIM-Version 2017.002, [R factor [N/h/yr] based on hourly rainfall series of RADKLIM, version 2017.002 (in German)], https://opendata.dwd.de/climate_environment/CDC/grids_germany/annual/erosivity/precip_radklim/2017_002/, last access: 15 May 2023, 2023.

Woodward, D.E., Hawkins, R.H., and Quan, Q.D.: Curve number method: Origins, applications and limitations, in: Hydrologic Modeling for the 21st Century: 2nd Federal Interagency Hydrologic Modeling Conf., Las Vegas, NV, http://ftp.bossintl.com/download/Runoff-Curve-Number-Method-Origins-Applications-and-Limitations.doc, 2002.

Rogler, H., Schwertmann, U.: Erosivität der Niederschläge und Isoerodentkarte Bayerns, [Erosivity of precipitation and iso-erosivity map for Bavaria], Z. Kulturtech. Flurberein. 22, 99–112, 1981.

Seibert, S. and Auerswald, K.: Hochwasserminderung im ländlichen Raum – Ein Handbuch zur quantitativen Planung, [Flood mitigation in rural areas – a handbook for quantitative planning (in German)], Springer Verlag, https://doi.org/10.1007/978-3-662-61033-6, 2020.

.